MODIS
Engineering Model Data
SDST Geolocation Analysis Report

November 15, 1995

SDST-045

MODIS
Engineering Model Data
SDST Geolocation Analysis Report

Prepared by:

_____

Frederick Patt, SAIC/GSC Date
SDST Geolocation Lead

Reviewed by:

_____

Jenny Glenn, SAIC/GSC Date
SDST System Analyst

_____

Laurie Schneider, SAIC/GSC Date
SDST R&QA Manager

_____

Thomas Piper, SAIC/GSC Date
MODIS SDST Task Leader

Approved by:

_____

Edward J. Masuoka, GSFC/Code 920.2 Date
MODIS SDST Manager

Change Record Page

This document is baselined and has been placed under Configuration Control. Any changes to this document will need the approval of the Configuration Control Board.

Document Title: MODIS Engineering Model Data SDST Geollocation Analysis Report

Document Date: November 15, 1995

Issue	Date	Page Affected	Description
Original	11/15/95	All	Baselined

MODIS
Engineering Model Data
SDST Geolocation Analysis Report

Table of Contents

1. INTRODUCTION 1
1.1 Purpose 1
1.2 Scope 1
1.3 Background 1
1.4 Applicable Documents 2
1.5 Organization of the Report 2

2. DATA FORMAT AND CONTENT 3
2.1 Engineering Model Data Format 3
2.1.1 Payload Interface Controller Record Format 3
2.1.2 MODIS Scan Data in the Payload Interface Controller Format 4
2.2 Engineering Model Test Data Set Characteristics 5

3. DATA ACCESS AND ANALYSIS PROCEDURES 8
3.1 Data Input 8
3.2 Data Extraction 8
3.2.1 MODIS Detector Data 8
3.2.2 Time codes 9
3.2.3 Mirror Encoder Data 9

4. RESULTS 10
4.1 Time Codes 10
4.2 Mirror Encoder Data 10
4.3 Detector Data 14

5. CONCLUSION 53

6. INTERACTIVE DATA LANGUAGE PROCEDURES USED FOR THE ENGINEERING MODEL DATA ANALYSIS 54
6.1 Data Input 54
6.2 MODIS Detector Data 54
6.3 Time Codes 55
6.4 Mirror Encoder Data 56

7. ACRONYMS 57

List of Figures

Figure 4-1 Packet Times Illustrating Normal Sequence 11
Figure 4-2 Packet Times Illustrating Time Code Anomaly 12
Figure 4-3 Scan-to-Scan Differences Between Time Codes 13
Figure 4-4 Mirror Encoder Data for One Scan 16
Figure 4-5 Mirror Encoder Differences for One Scan 17
Figure 4-6 Mirror Encoder Differences for 20 Scans Versus Sample Number 18
Figure 4-7 Band 12 Data for One Detector and Scan 20
Figure 4-8 Band 12 Data for Four Scans 21
Figure 4-9 Band 26 Data for Four Scans 22
Figure 4-10 Slit Observed in Three Samples 23
Figure 4-11 Slit Observed in Two Samples 24
Figure 4-12 Slit Center Locations for One Scan of Band 12 26
Figure 4-13 Slit Center Locations for Band 1 27
Figure 4-14 Slit Center Locations for Band 2 28
Figure 4-15 Slit Center Locations for Band 3 29
Figure 4-16 Slit Center Locations for Band 4 30
Figure 4-17 Slit Center Locations for Band 8 31
Figure 4-18 Slit Center Locations for Band 9 32
Figure 4-19 Slit Center Locations for Band 10 33
Figure 4-20 Slit Center Locations for Band 11 34
Figure 4-21 Slit Center Locations for Band 12 35
Figure 4-22 Slit Center Locations for Band 13 36
Figure 4-23 Slit Center Locations for Band 14 37
Figure 4-24 Slit Center Locations for Band 15 38
Figure 4-25 Slit Center Locations for Band 16 39
Figure 4-26 Slit Center Locations for Band 17 40
Figure 4-27 Slit Center Locations for Band 18 41
Figure 4-28 Slit Center Locations for Band 19 42
Figure 4-29 Slit Center Locations for Band 20 43
Figure 4-30 Slit Center Locations for Band 22 44
Figure 4-31 Slit Center Locations for Band 23 45
Figure 4-32 Slit Center Locations for Band 24 46
Figure 4-33 Slit Center Locations for Band 26 47
Figure 4-34 Slit Center Locations for Band 27 48
Figure 4-35 Slit Center Locations for Band 28 49
Figure 4-36 Slit Center Locations for Band 29 50

List of Tables

Table 2-1 PIC Record Format for MODIS Packets 4
Table 2-2 MODIS Scan Data in the PIC Format 5
Table 2-3 EM Test Data Set Characteristics 6
Table 4-1 Mirror Encoder Values and Successive Differences for One Scan 15
Table 4-2 Representative Signals and SNRs for Slit Data 51

MODIS
Engineering Model Data
SDST Geolocation Analysis Report

1. INTRODUCTION

1.1 Purpose

The purpose of this report is to describe the investigations and analysis of the Moderate Resolution Imaging Spectroradiometer (MODIS) Engineering Model (EM) data which have been performed by the MODIS Science Data Support Team (SDST) Geolocation Team. The data were collected during a series of performance tests carried out by Santa Barbara Research Corporation (SBRC) in the spring of 1995. The analysis of these data by the Geolocation Team is performed to verify and/or improve the algorithms and design for the geolocation software.

This analysis investigated four key areas:

1. Verify behavior of the time code is consistent with Contract Data Requirements List (CDRL) 305.

2. Perform a direct correlation between mirror motion and registration variations.

3. Assess the internal consistency of the image registration for each band.

4. Conduct a co-registration analysis.

The analysis may also be used to assess the completeness of the spatial verification test procedures used by SBRC to collect the data and to determine the need for modified or additional tests.

1.2 Scope

The investigations and analysis described in this document have been performed for the express purpose of contributing to the development of the MODIS geolocation software. They are not intended to serve the broader purpose of general MODIS instrument characterization or requirements verification. Therefore, the analyses described herein will have the specific goal of improving the Geolocation Team's knowledge of the instrument as it relates to the geolocation software design. However, the results may be of use to a broader audience, and so will be distributed to other interested persons within the MODIS Project.

1.3 Background

The MODIS instrument for the Earth Observing System (EOS) AM1 platform will be built and tested by SBRC in two versions: the EM and the protoflight unit. Each version will be run through a series of performance tests; the EM tests are a subset of the performance tests to be run on the protoflight instrument. The full scope of tests to be performed is described in CDRL 022 (see Section 1.5).

A specific set of instrument tests have been designated as system spatial performance tests. Various elements of these tests are performed under both ambient and thermal vacuum test conditions.

It is important to note that the MODIS EM is a completely separate physical unit from the protoflight unit. Therefore the results of EM data analysis are at best a general indicator of the expected results for future testing and in-flight performance.

1.4 Applicable Documents

- MODIS EM Data Analysis Plan for Geolocation, Draft, SAIC/GSC, 4/28/95.
- Moderate Resolution Imaging Spectroradiometer (MODIS) Program Performance Verification Plan and Performance Verification Specification, Hughes SBRC (CDRL 202, 9/94).
- Test Procedure for MODIS EM Thermal Vacuum, Hughes SBRC (Document Number E152807, Initial Release 3/95)
- Moderate Resolution Imaging Spectroradiometer (MODIS) Engineering Telemetry Description, Hughes SBRC (CDRL 305, 4/94; update pages 11/94).

1.5 Organization of this Report

The remainder of this report will be organized as follows.

- Section 2 will describe the format and content of the EM test data sets which have been received and examined.
- Section 3 will describe the procedures and software used for data access and analysis.
- Section 4 will present the analysis, methods, and results.
- Section 5 will discuss the conclusions reached from the analysis.
- Section 6 describes the sample Interactive Data Language (IDL) code for data access and analysis procedures.
- Appendix A is a list of the acronyms used in this document.

2. DATA FORMAT AND CONTENT

This section discusses both the detailed record format for the EM test data and the characteristics of the test data sets acquired.

2.1 Engineering Model Data Format

The EM test data acquired by the SDST have all been processed through the Payload Interface Controller (PIC) prior to being archived by SBRC. The PIC performs reformatting and subsetting of the MODIS data prior to making it available for archiving. The two questions which needed to be resolved to allow the analysis to proceed were: the specific PIC record format, and the total information available from each MODIS scan.

It is stated for the record that the MODIS SDST in particular, and probably the Goddard Space Flight Center (GSFC) MODIS Project in general, have never received sufficiently detailed information about the PIC format. The description presented here resulted from combining the incomplete information provided by SBRC with additional examination of the actual data sets.

2.1.1 Payload Interface Controller Record Format

The PIC data are all produced in a native (binary) format. Each PIC record consists of a complete MODIS packet, which has been reformatted, including the Consultative Committee for Space Data Systems (CCSDS) primary and secondary headers and the MODIS header. The reformatting consists of taking 12-bit segments and padding them with zeroes to a 16-bit wide field. In essence, each 12-bit segment is right-justified in a two-byte word. A MODIS long packet (day mode, engineering or memory dump) consists of 5,136 bits, or 428 12-bit segments; the PIC records are 428 two-byte words long, or 6,848 bits. (No short, or night mode, packets are present in the acquired EM data).

The motivation for this reformatting is clear for the MODIS raw detector data. The measurements themselves, and the checksum at the end of the packet, are aligned on 12-bit boundaries, and are offset from the start of the packet by an integral number of 12-bit segments. Thus the effect of the reformatting is to place the detector measurements right-justified in two-byte words, which greatly simplifies the problem of reading and interpreting individual measurements.

However, the reformatting has an adverse effect on the remaining data. Most of the other fields, including the headers, the engineering packet data and the memory dump packet data, are not 12-bit aligned in the raw data. As a result, these fields are somewhat garbled, although no information has been lost, and re-packing is required for proper interpretation. The fields of interest for this analysis which are affected include the CCSDS time code (CCSDS secondary header), the frame type flags and frame count (MODIS header) and the mirror encoder data (data field of engineering packet 2).

The record format for all packets is summarized in Table 2-1. A detailed description of the CCSDS packet format is given in CDRL 305.

Table 2-1 PIC Record Format for MODIS Packets
(Bit and word numbers are zero-base)

Packet Segment	MODIS Packet Bits	PIC Record Words
CCSDS Primary Header	0-47	0-3
CCSDS Secondary Header (Packet Time Code)	48-111	4-9 *
MODIS Header	112-143	9-11 *
MODIS Data Field	144-5123	12-426
MODIS Checksum	5124-5135	427

*-PIC word 9 spans the boundary between the CCSDS Secondary Header and the MODIS header.

2.1.2 MODIS Scan Data in the Payload Interface Controller Format

The PIC allowed the MODIS scan Earth view sector data to be reduced to a commandable subset of the frames collected for that sector. Otherwise, the EM data consisted of complete MODIS scans, with all sectors and data types included. The numbers of frames collected for each calibration sector are the same for all data acquired. In addition, each scan includes engineering and memory dump packets (two of each), as expected for the full MODIS data stream. This fact is crucial to the analysis of the mirror encoder data, which are contained in the second engineering packet. The packets and frames of each type are summarized in Table 2-2.

The length and position of the Earth view sector subset varied among the test sets. Most test sets included frames 650 through 700 (51 frames or 102 packets total). Two sets included frames 650 through 750, and one set included full Earth sectors of 1,354 frames. The specific Earth view sector length associated with each data set is described in Section 2.2.

The number of PIC records per scan thus depends on the length of the Earth sector subset. The combined calibration, engineering, and memory dump data require 324 records per scan. For a test data set with 51 Earth view frames, a total of 426 records are required per scan; for 1,354 Earth view frames 3,032 records are required.

Table 2-2 MODIS Scan Data in the PIC Format

Data Sector or Type	Number of Packets	Number of Frames
Solar Diffuser	100	50
Spectroradiometric Calibration Assembly (SRCA)	20	10
Black Body	100	50
Space View	100	50
Earth View	2N	N *
Engineering	2	n/a
Memory Dump	2	n/a

*-Subset of Earth sector varies from 51 to 1354 frames.

2.2 Engineering Model Test Data Set Characteristics

The EM data acquired for this analysis were collected during the spatial characterization tests. The test procedures for the various test phases are described in CDRL 202. The spatial tests included two overall types of tests, which are distinguished by the MODIS scan mirror being in either dynamic or static mode. As discussed in the EM Data Analysis Plan, this analysis utilizes the dynamic mode data.

The EM test data sets acquired can be categorized as follows: number of Earth sector frames; number of scans per file; bands collecting useful data; target; and test phase (ambient or thermal vacuum). Each data set was assigned a Unique Acquisition Identification (UAID) number by SBRC, which uniquely identifies the test and data collection. For each UAID, a number of data files were collected (ranging from 5 to 28 in the acquired data). The overall data characteristics are constant for the UAID, but other test conditions (such as target position) may be varied among data files.

The characteristics of the acquired data sets (shown in Table 2-3) were determined from a combination of SBRC test reports and examination of the files themselves. As can be seen from the table, the majority of the UAIDs have 51 Earth view frames and 20 scans per file. The target in all of the test sets consisted of either a narrow slit (less than one sample in width, observed in two consecutive samples) or a wide slit (observed in three or more consecutive samples). Within a UAID, the target is typically moved along-scan by a small amount (e.g., 0.1 sample) between files.

Table 2-3 EM Test Data Set Characteristics

UAID	Earth View Frames	Scans per File	Number of Files	Useful Bands	Target	Test Phase
257	650-700	50	21	1-4, 8-12	n. slit	Amb.
290	650-700	20	10	1-4, 8-12	n. slit	Amb.
291	650-700	20	10	1-4, 8-12	n. slit	Amb.
292	650-700	20	10	1-4, 8-12	n. slit	Amb.
293	1-1354	20	10	1-4, 8-12	n. slit	Amb.
294	650-700	20	10	1-4, 8-12	n. slit	Amb.
383	650-750	20	28	22, 23, 24, 27, 28	w. slit	Amb.
384	650-750	20	6	22, 23, 24, 27, 28	w. slit	Amb.
414	650-700	20	10	1-4, 8-16, 22-24, 26	n. slit	T/V
415	650-700	20	5	1-4, 8-16, 22-24, 26	n. slit	T/V
417	650-700	20	5	1-4, 8-16, 22-24, 26	n. slit	T/V
465	650-700	20	10	1-4, 8-20, 22-24, 26-29	n. slit	T/V
466	650-700	20	10	1-4, 8-20, 22-24, 26-29	n. slit	T/V
467	650-700	20	10	1-4, 8-12, 17-20, 22-24, 26-29	n. slit	T/V

Notes:

Targets: N. slit - narrow slit
W. slit- wide slit

Test Phases: Amb.-Ambient Test
T/V-Thermal Vaccum Test

The determination of the useful bands for each UAID has been difficult, and is still in progress as of this date; in several cases it has been problematic to reconcile the SBRC test records with the apparent results in the data itself. Much of this effort has involved plotting the detector data to determine whether the target was observed and if the background signal level was stable enough to allow the data to be used for spatial registration analysis.

Several bands do not appear to produce useful data in any of the tests. Noteworthy among these are the near-infrared 500 m bands (5-7) for which the two samples generated per frame consistently have significantly different values, and most at the long-wave infrared bands (30-36), which do not produce a perceptible signal from the target in any of the data sets acquired. This problem appears to eliminate the possibility of analyzing these bands for spatial effects.

It is also noteworthy that, in some cases, a series of UAIDs will have apparently identical test characteristics. This is true, for example, of UAIDs 290, 291, 292, and 294.

3. DATA ACCESS AND ANALYSIS PROCEDURES

The EM data access and analysis has been performed entirely using the IDL by Research Systems, Inc. The IDL has the capability to read the binary data records, manipulate the data, and generate graphics displays (on screen or hardcopy). It is well suited to this type of analysis. The following sections discuss the procedures for data input and extraction. Sample IDL code for these procedures is given in Section 6.

3.1 Data Input

The EM data were input to IDL via an unformatted read into an internal 3-dimensional array of short (16-bit) integers. This data type was determined by the two-byte alignment of the PIC data. The array dimensions are determined by the record length and test data set characteristics as discussed in Section 2. The first array dimension is set by the PIC record length of 428 words. The second and third dimensions depend on the Earth sector size and the number of scans, respectively. For example, to read in a single file with 51 Earth view frames and 20 scans would require an array with dimensions (428,426,20). The memory capacity of modern computer workstations can accommodate several such arrays, allowing multiple files to be read and analyzed simultaneously, and even the largest files (~50 Mbytes) are readily input. Sample code for the data input is shown in Section 6.

3.2 Data Extraction

As stated previously, the two-byte alignment of the PIC data is well suited to the analysis of the MODIS detector data, but additional effort is required to extract other data fields. In the following subsections the procedures for extracting the detector data, time codes, and mirror encoder data are discussed.

3.2.1 MODIS Detector Data

The MODIS detector data have already been 16-bit aligned by the PIC, so the extraction of data for a selected band is a simple re-ordering of the data. The order of data samples in the MODIS packet is given in CDRL 305. As specified, all of the samples associated with a given 1-km spatial element are stored in 83 contiguous 16-bit words in the data, with each record containing data for five spatial elements. Within the 83 words, 0-31 are Bands 1 and 2 (250m), 32-51 are Bands 3 through 7 (500m) and 52-82 are Bands 8 through 36 (1 km).

For the 1 km bands the extraction of a band simply involves indexing to the first sample in the record for that band and then to every 83rd word for the remaining samples. This is performed for two consecutive records to obtain a single frame of data.

For the 250m and 500m bands, the extraction is a two-step process; first the samples for the band are extracted in order as in the data, and then resorted by detector, sample, and frame.

The IDL procedure for band data extraction is shown in Section 6.

3.2.2 Time codes

The CCSDS packet segmented time code for EOS AM1 (described in CRDL 305) is a 64-bit field, which consists of a day count (16 bits), milliseconds of day (32 bits), and microseconds of millisecond (16 bits). The PIC reformatting results in the packet time codes being arranged as follows:

- Day count: word 4, bits 4-15; and word 5, bits 4-7
- Milliseconds: word 5, bits 8-15; word 6, bits 4-15; and word 7, bits 4-15
- Microseconds: word 8, bits 4-15; and word 9, bits 4-7

The determination of the time codes involves extraction, shifting, and addition of the appropriated bits from the PIC words to eliminate the pad bits and reconstruct each field. IDL code to perform this is given in Section 6.

3.2.3 Mirror Encoder Data

The mirror encoder data (referred to as Earth Encoder Times in CDRL 305) are contained in the second engineering packet, which is transmitted as the third-to-last packet in each scan; for a scan containing 426 packets the encoder data would be contained in packet 423. The encoder data are the first segment in the MODIS data field of the packet, and are generated by the instrument as a series of 24 contiguous 16-bit integers. The PIC reformatting (12-bit to two-byte) causes 4 pad bits to be inserted before each set of 12 bits. As a result, each set of three encoder words is distributed across four PIC words, as shown here for the first three encoder words:

- Encoder word 1: word 12, bits 4-15; and word 13, bits 4-7
- Encoder word 2: word 13, bits 8-15; and word 14, bits 4-11
- Encoder word 3: word 14, bits 12-15; and word 15, bits 4-15

This sequence is repeated for the remaining 21 encoder words and 28 PIC words. The IDL code to reconstruct the encoder data is shown in Section 6.

4. RESULTS

The following subsections describe the analysis and results for the time codes, mirror encoder data, and useful band data.

4.1 Time Codes

The time codes behave as expected overall. As specified, all of the packets for a sector have the same time code, and the increment between sectors is essentially as expected. Two anomalies have been found, one major and one minor.

The normal sequence of packet times is illustrated in a plot of the milliseconds-of-day versus packet number for two successive scans in one of the data files (Figure 4-1). The plot shows the times for the five sectors (solar diffuser, SRCA, blackbody, space view, and Earth view) in each scan, with the time being the same for all of the packets in a scan. The relative timing of the sectors is essentially identical for the two scans.

Periodically a large anomaly occurs in the sequence of sector times, which is seen as one of the sectors being out of time sequence. This appears to result from an offset of about 1 second in the sector time code. The anomaly is seen in another plot of time codes for two different scans in the same file (Figure 4-2). In this case the times for the third sector, which is the blackbody sector from the first scan, is clearly out of sequence. The time sequence is otherwise nominal for the remaining sectors.

This anomaly occurs regularly throughout the EM data. It has been observed for several sectors in every file for which time codes have been examined, and in all types of sectors at various times.

The minor anomaly is that the difference in the time codes for successive scans deviates from the expected value of about 1,477 milliseconds, by up to 28 milliseconds. The differences all fall into a few discrete groups, none of which includes 1,477 milliseconds. This effect can be seen in a plot of scan-to-scan time code differences for all sector types (Figure 4-3). The plot shows that the differences are all grouped around 1,449, 1,465, 1,481, and 1,498.

4.2 Mirror Encoder Data

The mirror encoder data (referred to as Earth Encoder Times in SBRC documentation) consist of 24 two-byte integers per scan. They are defined in CDRL 305, Table 30-5A as "Time between every 100th mirror encoder pulse over earth view". Table note 2 gives the nominal value as 18,032 microseconds, which is consistent with the nominal MODIS scan interval of 1.4772 seconds.

The mirror encoder data in the EM test data are not consistent with the SBRC specifications. Most of the values appear to contain total accumulated time of every 100th encoder pulse from a starting point, rather than incremental time as specified. Given the range of a two-byte integer, the value rolls over every three or four samples. In addition, the first two samples and the last sample per scan are not consistent with either incremental or accumulated time.

Figure 4-1 Packet Times Illustrating Normal Sequence

Figure 4-2 Packet Times Illustrating Time Code Anomaly

Figure 4-3 Scan-to-Scan Differences Between Time Codes

The behavior of the encoder can be seen in a plot of one scan of data (Figure 4-4). The first encoder sample per scan is always zero. The second sample has an (apparently) arbitrary value which changes from scan to scan. The third through 23rd sample each differ from the previous sample by about 18,032 counts (except for rollovers). The last sample differs from the previous sample by 36,061 counts, or about twice the normal value.

The rollover appears to occur at 64,000 counts, rather than 65,536 as would be expected for an unsigned two-byte integer. When corrected for rollover at this value, nearly all of the successive differences are close to the nominal value of 18,032 counts. This is shown by tabulating the encoder values, successive differences and differences corrected for rollover at 64,000 (Table 4-1). All but the first and last differences are within a few counts of 18,032.

A plot of the differences for samples 2 through 22 (Figure 4-5) shows the small deviation from the nominal value, and also shows some apparent periodic behavior across the scan. Overplotting differences for all scans versus sample number (Figure 4-6) shows that this periodic behavior is consistent in all scans and that the variation among scans is only 1 or 2 microseconds, which is insignificant compared with the 333 microsecond sampling period of the MODIS 1 km bands. If the scan mirror rotation rate is as stable as this plot seems to indicate, then scan mirror variations should not contribute significantly to geolocation errors. However, given the difficulty and uncertainty in interpreting the EM mirror encoder data, it is not possible to draw clear conclusions.

In addition, several points on this plot fall well outside the typical values, with differences about 25 microseconds above the nominal value; this constitutes yet another anomaly in the encoder data which cannot be reconciled with the SBRC specifications.

In summary, the mirror encoder data in the EM test data sets are not consistent with the SBRC specifications, and we do not have a model that allows consistent interpretation of all of the encoder samples. The analysis originally proposed for the encoder data will not be possible, and explanation and/or correction from SBRC are required.

4.3 Detector Data

The motivation for analyzing the detector data was to assess the internal consistency of the image registration for each band and to perform band-to-band comparisons. The narrow slit target, which was used for the majority of the test data sets, was well suited for the purpose of determining along-scan co-registration. The original intent was also to attempt a direct correlation between the mirror motion and registration variations; due to the problems found with the mirror encoder data this correlation will not be possible. This section presents the methods and results of the analyses performed on the detector data.

Table 4-1 Mirror Encoder Values and Successive Differences for One Scan

Sample Number	Value	Difference	Difference with rollover correction
0	0	n/a	n/a
1	8944	8944	8944
2	26974	18030	18030
3	45004	18030	18030
4	63035	18031	18031
5	17069	-45966	18034
6	35099	18030	18030
7	53130	18031	18031
8	7159	-45971	18029
9	25190	18031	18031
10	43224	18034	18034
11	61255	18031	18031
12	15287	-45968	18032
13	33317	18030	18030
14	51347	18030	18030
15	5380	-45967	18033
16	23412	18032	18032
17	41444	18032	18032
18	59472	18028	18028
19	13504	-45968	18032
20	31535	18031	18031
21	49567	18032	18032
22	3599	-45968	18032
23	39660	36061	36061

Figure 4-4 Mirror Encoder Data for One Scan

Figure 4-5 Mirror Encoder Differences for One Scan

Figure 4-6 Mirror Encoder Differences for 20 Scans Versus Sample Number

As discussed in Section 3, most of the test sets were collected with nearly identical characteristics. In order to perform co-registration analysis among bands, a few sets were needed that contained useful data for the largest number of bands. The criteria were: consistent background signal, signal level observed for the slit, and lack of saturation. The additional frames included with UAIDs 293, 383, and 384 provide no additional information, since the target was always observed within the range of frames 650-700.

Two data sets were chosen for the analysis based upon the characteristics described in Table 2-3 and on an extensive analysis of the data. They were: UAID 467 for bands 1-4, 8-12, 17-20, 23-24, and 26-28; and UAID 465 for bands 13-16. Overall, these sets contained useful data for the largest number of bands. Ideally one UAID would have been useful for all bands; however, bands 13-16 exhibited "clipping" of the signal in UAID 467, and the short wavelength bands (3, 4, 8, and 9) had low signal-to-noise ratios (SNRs) in UAIDs 465 and 466.

To illustrate the types of detector outputs observed in the test data and the analysis methods, we used Band 12 data, which had uniformly good signals and SNRs. The procedures in Section 3.2 were used to extract Band 12 data for one file (20 scans) of UAID 467. A plot of the first scan and detector (Figure 4-7) shows that the slit used as the target for this test was observed in frames 679 and 680. A surface plot for the first 4 scans (Figure 4-8) shows a stable background signal and some variation among the 10 detectors in the peak signal produced by the slit.

Several of the bands were not as well behaved as Band 12. In particular, the medium and long-wave infrared bands showed much greater variability in the background and the slit signal level. This is illustrated in a surface plot for 4 scans of Band 26 (Figure 4-9). This figure shows dramatic variations in the slit signal among the 10 detectors, and the background not only varies among detectors but also changes significantly at the ends of the scan range. However, the behavior appears to be quite consistent from scan to scan, and the slit signal produced by each detector is quite clear.

Using a simple model for the signal produced by scanning a narrow slit, these measurements can be used to estimate the relative along-scan position of the 10 detectors and the scan-to-scan stability in these positions. For a triangular response weighting function, the output for the samples which observed the slit can be modeled as follows. A slit target which is narrower than the nominal sample width can be observed in either two or three consecutive samples. For the case of three samples (Figure 4-10), the slit is located close to the center of the response weighting function for the second sample and at the edges of the first and third samples.

Figure 4-7 Band 12 Data for One Detector and Scan

Figure 4-8 Band 12 Data for Four Scans

Figure 4-9 Band 26 Data for Four Scans

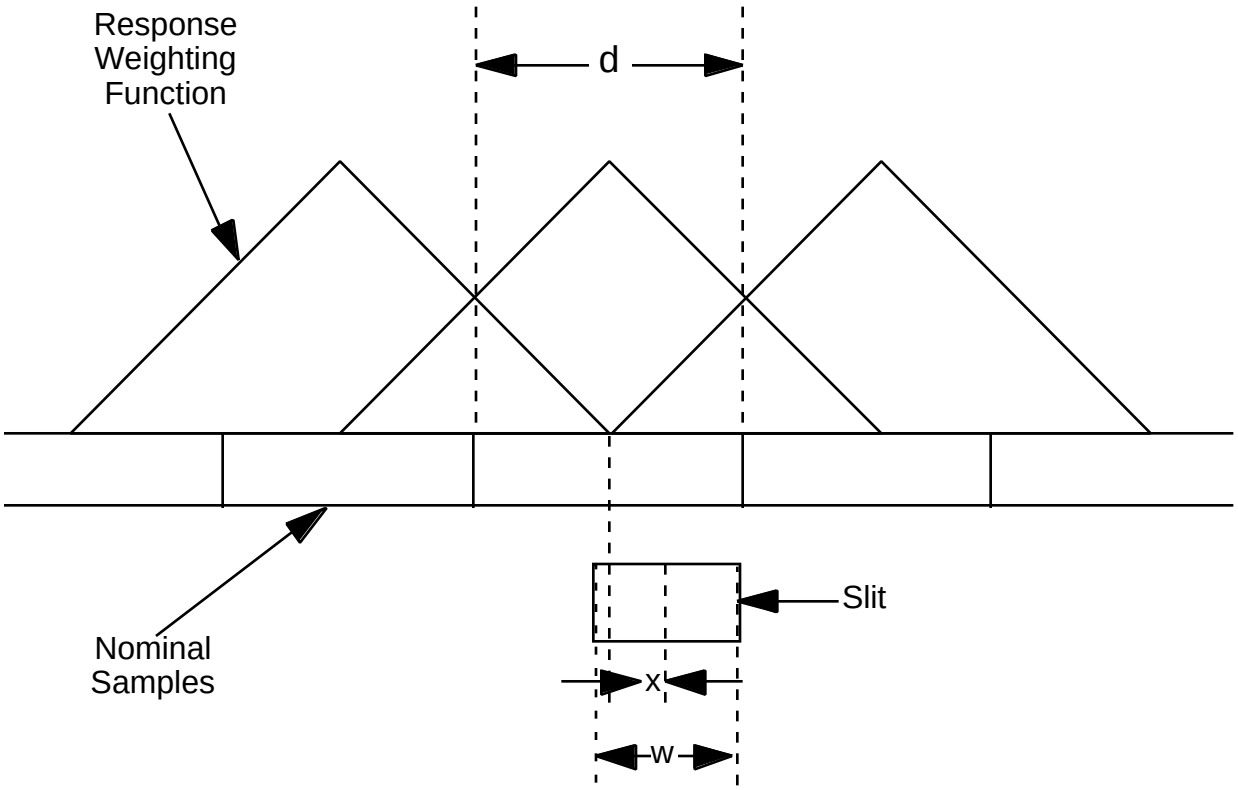

Figure 4-10 Slit Observed in Three Samples

If the slit center is offset by an amount X from the center of the second sample, the signal observed in the first sample is:

$$S1 = 0.5*R*(W/2-X)^2 \quad \text{[equation 1]}$$

where S1 is the signal (corrected for the background level), R is the slit radiance, and W is the slit width. The units of S1 and R are arbitrary. Likewise, the signal from the third sample is:

$$S3 = 0.5*R*(W/2 + X)^2 \quad \text{[equation 2]}$$

and from the second sample is:

$$S2 = R*(W*D-0.25*W^2-X^2) \quad \text{[equation 3]}$$

where D is the detector, or sample, width. The total signal from the three samples is R*D*W, or the product of the slit radiance, slit width, and detector widths, as expected. These expressions are valid for |X| < W/2. If the difference between the third and first samples is divided by the sum of all three samples, the result is:

$$(S3-S1)/(S1 + S2 + S3) = (R*W*X)/(R*W*D) = X/D \quad \text{[equation 4]}$$

which is the slit center offset from the second sample center, expressed as a fraction of the sample width. This is a very useful result since it is independent of the slit radiance and width.

If |X| > W/2, then the slit is observed in two samples (Figure 4-11). For positive X, S1 = 0, and the values of S2 and S3 are as follows:

$$S2 = R*W*(D-X) \quad \text{[equation 5]}$$

$$S3 = R*W*X \quad \text{[equation 6]}$$

For negative X, S3 = 0, and

$$S1 = -R*W*X \quad \text{[equation 7]}$$

$$S2 = R*W*(D + X) \quad \text{[equation 8]}$$

In both cases, Equation 4 still produces the desired result: X/D.

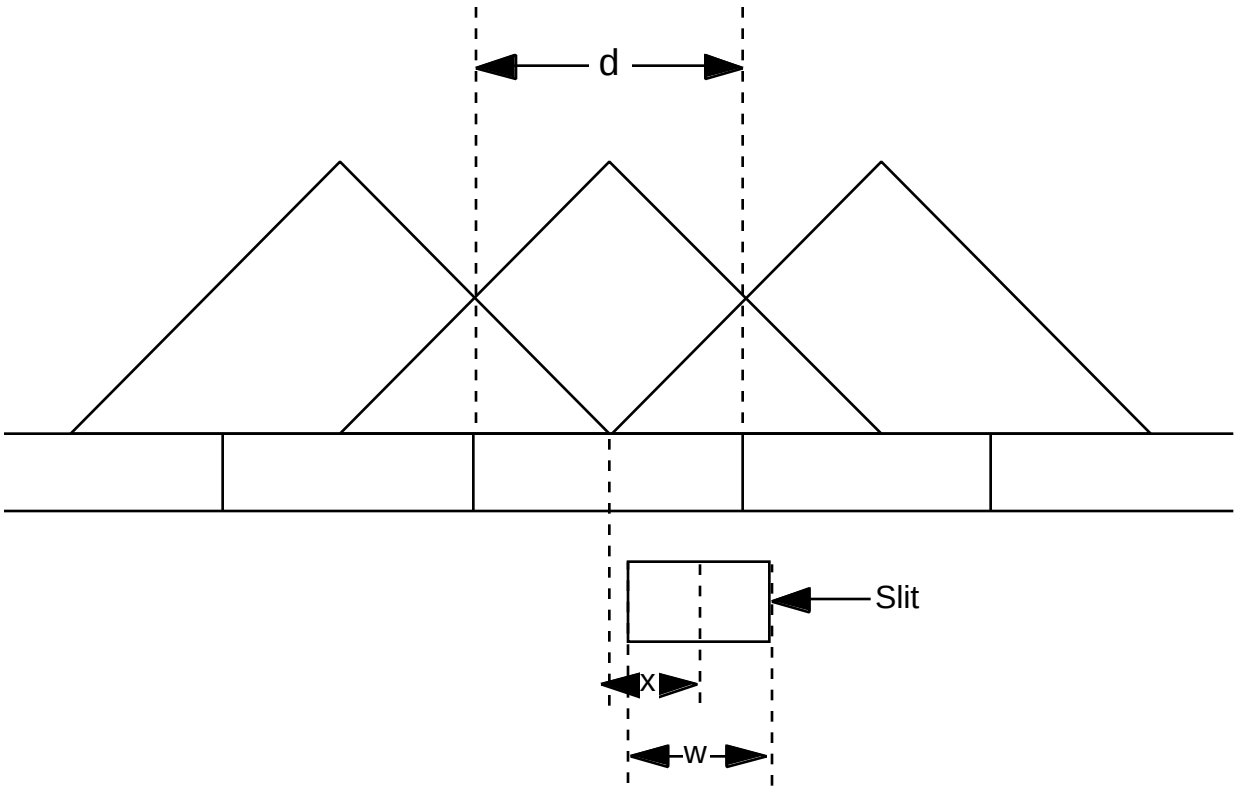

Figure 4-11 Slit Observed in Two Samples

This method assumes that S2 always has a larger magnitude than S3 or S1. In practice it requires finding the sample with the largest signal and using this for S2. The result of Equation 4 is then added to the sample number to get the slit position within the scan. In practice, the quality of the results produced by this method for a particular band and detector will be affected by deviations of the response weighting function from the ideal triangular form and by the noise levels in the data.

Initially the method was applied to Band 12 data for the 20 scans contained in the first file of UAID 467, and the results plotted (Figure 4-12). Each group of 10 symbols represents the values for the 10 detectors and one scan. The pattern for the scan group is very repetitive, with the spread among the detectors being quite small (about 0.005 IFOV). The scan-to-scan variations can also be seen clearly, with a range of about 0.04 IFOV. The alternating scans represent mirror sides 1 and 2, and the average difference between the two sides is clearly visible. For the data collected from a single mirror side the range is about 0.02 IFOV, which is equivalent to a scan mirror angle variation of about 3 arcseconds. This is of the same order as the variability in the scan mirror rate, which is suggested by the results discussed in Section 4.2.

This method was applied to all of the bands listed above (1-4, 8-20, 22-24, and 26-29) using data from either UAID 465 or 467. Both of these data sets contained 10 files of 20 scans each. The results of these calculations were shown by plotting computed slit locations vs. scan line number for all 10 files (Figures 4-13 to 4-36). For the high resolution bands, the slit center sample number was converted to an equivalent frame number by dividing by the number of samples per frame, to allow these results to be compared with those from the other bands. In the case of Bands 13 and 14, the two outputs (high and low gain) each produced essentially identical results, so only one set was included.

Two results are immediately apparent: the change in target position of 0.1 IFOV between files is clearly reflected in the computed slit positions; and the results for each target position are very similar to those shown in Figure 4-12 for most of the bands. Most of bands also exhibit a unique pattern in the relative positions of the ten detectors for a scan, and this pattern is repeated consistently for every scan and file, shifted according to changes in the mirror motion and target position.

The medium and long-wave bands (20, 22-24, and 26-29) show less consistency and more noise than the other bands. In most of these, the average slit locations for each slit position can be seen in the plot, but with numerous outliers and greater variability in the relative detector locations. For Band 29, the scatter is large enough to obliterate any pattern in the results.

Figure 4-12 Slit Center Locations for One Scan of Band 12

Figure 4-13 Slit Center Locations for Band 1

Figure 4-14 Slit Center Locations for Band 2

Figure 4-15 Slit Center Locations for Band 3

Figure 4-16 Slit Center Locations for Band 4

Figure 4-17 Slit Center Locations for Band 8

Figure 4-18 Slit Center Locations for Band 9

Figure 4-19 Slit Center Locations for Band 10

Figure 4-20 Slit Center Locations for Band 11

Figure 4-21 Slit Center Locations for Band 12

Figure 4-22 Slit Center Locations for Band 13

Figure 4-23 Slit Center Locations for Band 14

Figure 4-24 Slit Center Locations for Band 15

Figure 4-25 Slit Center Locations for Band 16

Figure 4-26 Slit Center Locations for Band 17

Figure 4-27 Slit Center Locations for Band 18

Figure 4-28 Slit Center Locations for Band 19

Figure 4-29 Slit Center Locations for Band 20

Figure 4-30 Slit Center Locations for Band 22

Figure 4-31 Slit Center Locations for Band 23

Figure 4-32 Slit Center Locations for Band 24

Figure 4-33 Slit Center Locations for Band 26

Figure 4-34 Slit Center Locations for Band 27

Figure 4-35 Slit Center Locations for Band 28

Figure 4-36 Slit Center Locations for Band 29

As stated above, the consistency of the results is dependent upon the signal-to-noise ration (SNR) for the data; therefore it should be possible to correlate the scatter shown in the plots with the SNRs for each band. Representative SNRs were computed as follows. The total signal observed for the slit was determined by adding the three slit observation samples as in the denominator of Equation 4. The average background level was computed using the 10 samples preceding and following the slit samples, and the signal noise level was estimated as the standard deviation of these samples. (Note that the samples outside of this range could not be used for the longer wavelengths due to the change in the observed background signal as shown in Figure 4-9.) The SNR is the ratio of the slit signal to the background standard deviation. The results for the bands are given in Table 4-2.

Table 4-2 Representative Signals and SNRs for Slit Data

Band	Background Level	Noise Level	Slit Signal	Signal-to-Noise Ratio
1	222.850	3.81514	1232.45	323.042
2	225.550	3.28433	1666.35	507.363
3	225.100	0.911909	272.700	299.043
4	222.450	1.09904	718.650	653.887
8	219.050	0.394034	145.850	370.145
9	215.500	0.606977	387.500	638.410
10	220.700	0.801315	1069.90	1335.18
11	220.300	1.71985	1994.10	1159.46
12	224.950	2.62528	2636.15	1004.14
13	244.200	1.10501	1031.40	933.383
14	229.650	1.30888	1364.05	1042.15
15	234.550	1.70062	1878.35	1104.51
16	225.250	1.06992	938.250	876.932
17	213.950	0.759155	119.150	156.951
18	218.000	0.458831	83.0000	180.894
19	227.800	1.05631	116.600	110.384
20	1191.85	6.52344	1482.45	227.250
22	1443.90	12.4600	1431.30	114.871
23	1482.70	5.24254	1494.90	285.148
24	1887.10	8.57720	1355.70	158.059
26	1931.45	8.04903	1509.65	187.557
27	2390.30	3.81272	227.100	59.5637
28	2474.05	4.95745	334.850	67.5447
29	2363.20	2.41922	70.4004	29.1004

As expected, all of the medium and long-wave bands had relatively high noise levels and low SNRs, with Band 29 having by far the lowest SNR. Most of the visible and short-wave bands had noise levels close to unity; Bands 11 and 12 have slightly larger noise levels but also have correspondingly large signal levels. Bands 1 and 2 also had larger noise levels; this resulted from variations in the background signal levels among the samples within each frame.

The plots show other systematic effects which merit additional analysis and explanation. The computed slit locations for several of the bands (2, 4, 22, 23, 24) included numerous outliers at regular intervals, most frequently for the first or last detector within a scan. Examination of the detector data for these bands shows a large incidence of anomalous values for the first and last detectors. For example, in the case of Band 2, the last sample of Detector 40 in each frame had a significantly larger value than all of the other values in the frame. In a few of the bands, one detector produced no apparent signal from the slit.

There is also a strong correlation among the results produced by the bands for a given focal plane. Comparison of Bands 1, 2, and 13 though 19 (near IR focal plane) shows that the average computed slit locations for all of these bands are very consistent. Likewise, Bands 3, 4, and 8 through 12 (visible) show very consistent results. However, there is a consistent offset in the average locations between the two groups, of about 0.05 IFOV. The results for Bands 20 through 24 appear to be offset from 0.15 to 0.2 IFOV from the visible Bands (although overall less consistent), while Bands 27 through 29 are offset by approximately 1.1 IFOV. This indicates that the consistency of detector registration within a focal plane is very good, with most of the differences between bands resulting from offsets between focal planes. An obvious exception is Band 26, which is offset by 5 IFOV. Since the value is equal to the position offset of this band on the focal plane, it appears that time shifting of the samples was not performed for Band 26 in the EM. In addition, there is a trend in the relative detector positions for a given band and scan which correlates with focal plane; all of the visible bands have a downward trend within a scan, while the near IR bands have an upward trend.

Finally, the correlation with mirror side is apparent in all but the noisiest bands, with mirror side 2 consistently producing slightly larger results than side 1. Analysis of the average side 2/side 1 differences for several bands shows this difference to be between 0.016 and 0.017 IFOV. This corresponds to a mirror wedge angle of about 2.5 arcseconds.

In general, these results show very good consistency both for a given band and between bands on the same focal plane with the obvious exception of Band 26. The differences discussed in the preceding paragraphs are well within expectations, and would have neglible impact on geolocation processing with the flight data.

5. CONCLUSION

This report concludes the analysis of the MODIS Engineering Model dynamic spatial registration data. The format and content of the data are well understood, and tools have been developed for extraction and analysis of the data. The results show anomalies in the time code and serious specification inconsistencies with the mirror encoder data. The latter will prevent completion of a principal objective of this analysis, the quantitative analysis of the mirror scan rate variability.

The detector radiances in the test data were used to perform along-scan spatial registration analysis of the visible, near-IR, and a few of the medium and long-wave IR bands. The analysis was performed by computing the along-scan location of a narrow slit target observed during the tests. The results show very good consistency both for a given band and among all of the bands analyzed, with both static and dynamic variations well within expected limits. In a few of the long-wave bands, the noise levels in the data rendered the results inconclusive. In addition, artifacts were observed in the results which were traced to anomalies in the detector data.

The methods described can be used to repeat these analyses with the protoflight model test data. However, in order to produce co-registration results for use in geolocation processing, three issues will need to be addressed in the protoflight model testing: 1) The targets used will need to support cross-scan as well as along-scan registration analysis; 2) Data will need to be collected using a target or targets which are visible in all MODIS bands; and 3) The problem with the interpretation of the mirror encoder data must be resolved, either by a change in the data itself or by a specification which allows meaningful interpretation.

6. INTERACTIVE DATA LANGUAGE PROCEDURES USED FOR THE ENGINEERING MODEL DATA ANALYSIS

6.1 Data Input

The following is an example of IDL statements for reading EM binary data. This example will open and read an EM data file named "1.dat" which contains 20 scans of data and has 51 Earth view frames per scan.

```
openr,1,'1.dat'             ; Open file for read-only access
data = intarr(428,426,20)  ;Define short integer array to hold
                            data
                           ;First dimension is packet size (fixed
                            for all data)
                           ;Second is total packets per scan
                           ;Third is number of scans

readu,1,data                ; Read unformatted data into array
                           ; End of IDL statements
```

6.2 MODIS Detector Data

The following is an IDL procedure for extracting a specified band from EM data which have been read into an IDL array.

```
pro get_band,data,iband,nscans,npix,band
; This is an IDL procedure for extracting detector samples
; from MODIS test data which have been re-formatted 12-bits to 2-
      bytes
; For 1 km bands
if (iband gt 7) then begin

; Define temporary array for data
     b = intarr(10,npix,nscans)

; Compute indices into record for band data
     in = indgen(5)*83 + iband + 56

; Extract band data into temporary array
     b(*,*,*) = data(in,320:(320+2*npix-1),0:nscans-1)

; Re-sort data into along-scan by along-track
     band = intarr(npix,10*nscans)
     for i=0,npix-1 do band(i,*) = b(*,i,*)

; For 500 m bands
endif else if (iband gt 2) then begin

; Define temporary array for data
     b = intarr(2,2,10,npix,nscans)
```

```
; Compute indices into record for band data
     in = indgen(5)*83 + (iband-3)*4 + 44

; Extract band data into temporary array
for i=0,1 do begin
for j=0,1 do begin
b(j,i,*,*,*) = data(in+j+2*i,320:(320+2*npix-1),0:nscans-1) endfor
endfor

; Re-sort data into along-scan by along-track
     band = intarr(2*npix,20*nscans)
     for i=0,npix-1 do for j=0,1 do band(2*i+j,*) = b(*,j,*,i,*)

; For 250 m bands
endif else begin

; Define temporary array for data
     b = intarr(4,4,10,npix,nscans)

; Compute indices into record for band data
     in = indgen(5)*83 + (iband-1)*16 + 12

; Extract band data into temporary array
     for i=0,3 do begin
     for j=0,3 do begin
     b(j,i,*,*,*) = data(in+j+4*i,320:(320+2*npix-1),0:nscans-1)
      endfor
     endfor

; Re-sort data into along-scan by along-track
     band = intarr(4*npix,40*nscans)
     for i=0,npix-1 do for j=0,3 do band(4*i+j,*) = b(*,j,*,i,*)

endelse

return
end                          ; End of IDL procedure
```

6.3 Time Codes

The following is an IDL procedure for extracting CCSDS time codes (day, milliseconds, microseconds) from EM data which have been read into an IDL array.

```
pro get_time, data, nscans, day, msec, micro

; This is an IDL procedure for extracting CCSDS packet times
; from MODIS test data which have been re-formatted 12-bits to
; 2-bytes

; Construct day field from bits 4-15 of word 4 and bits 4-7 of
  word 5. day = data(4,*,*)*16 + data(5,*,*)/256
```

```
; Construct milliseconds field from bits 8-15 of word 5,
; bits 4-15 of word 6 and bits 4-15 of word 7
; Remember this is a long integer
msec = (data(5,*,*) mod 256)*16777216 + data(6,*,*)*long(4096) +
  data(7,*,*)

; Construct microseconds field from bits 4-15 of word 8 and bits
  4-7 of word 9. micro = data(8,*,*)*16 + data(9,*,*)/256

return
end                          ; End of IDL procedure
```

6.4 Mirror Encoder Data

The following is an IDL procedure for extracting MODIS mirror encoder data from EM data which have been read into an IDL array.

```
pro get_mirr,data,nscans,nefram,mirr,dmir

; This is an IDL procedure for extracting MODIS mirror encoder
; times from MODIS test data which have been re-formatted 12-bits
; to 2-bytes

; Compute 2nd engineering packet number based on number of Earth
  view frames epkt2 = 321 + 2*nefram

; Move words containing encoder data to a temporary array b =
  data(12:43,epkt2,0:nscans-1)

; Define output array for encoder data
; (use long integer to avoid sign problems)
; mirr = lonarr(24,nscans)

; Define input and output array indices for encoder samples in =
  indgen(8)*4 ; Input array
  im = indgen(8)*3 ; Output array

; Reconstruct unsigned 16-bit encoder samples from input words
  mirr(im,*) = b(in,0,*)*long(16) + b(in+1,0,*)/256 mirr(im+1,*) =
  (b(in+1,0,*) mod 256)*long(256) + b(in+2,0,*)/16 mirr(im+2,*) =
  (b(in+2,0,*) mod 16)*long(4096) + b(in+3,0,*)

; Compute differences of successive encoder samples within a scan
  dmir = mirr(1:23,*)-mirr(0:22,*)

; Correct for rollover at encoder value of 64000
  nm = where(dmir lt 0)
  dmir(nm) = dmir(nm) + 64000

return
end                          ; End of IDL procedure
```

7. ACRONYMS

CCSDS	Consultative Committee for Space Data Systems
CDRL	Contract Data Requirements List
EM	Engineering Model
EOS	Earth Observing System
GSFC	Goddard Space Flight Center
IDL	Interactive Data Language
IFOV	Instaneous Field-Of-View
MODIS	Moderate Resolution Imaging Spectroradiometer
PIC	Payload Interface Controller
SBRC	Santa Barbara Research Corporation
SDST	Science Data Support Team
SNR	Signal-to-Noise Ratio
SRCA	Spectroradiometric Calibration Assembly
T/V	Thermal Vacuum
UAID	Unique Acquisition Identification